

The C and N abundances in disk stars^{*}

J. R. Shi^{1,2}, G. Zhao¹, and Y. Q. Chen¹

¹ National Astronomical Observatories, Chinese Academy of Sciences, Beijing 100012, PR China

² Chinese Academy of Sciences – Peking University Joint Beijing Astrophysical Center, Beijing 100871, PR China

Received 31 May 2001 / Accepted 29 October 2001

Abstract. Abundance analysis of carbon and nitrogen has been performed for a sample of 90 F and G type main-sequence disk stars with a metallicity range of $-1.0 < [\text{Fe}/\text{H}] < +0.2$ using the C I and N I lines. We confirm a moderate carbon excess in the most metal-poor disk dwarfs found in previous investigations. Our results suggest that carbon is enriched by superwinds of metal-rich massive stars at the beginning of the disk evolution, while a significant amount of carbon is contributed by low-mass stars in the late stage. The observed behavior of $[\text{N}/\text{Fe}]$ is about solar in the disk stars, irrespective of the metallicity. This result suggests that nitrogen is produced mostly by intermediate-mass stars.

Key words. stars: abundances – stars: late-type – Galaxy: evolution – Galaxy: solar neighbourhood

1. Introduction

Carbon and nitrogen are two of the most abundant heavy elements and they play key roles in the chain of nucleosynthesis. Accurate knowledge of the abundances of these elements in stellar atmospheres is of considerable astrophysical interest. The main nuclear processes that generate these two elements are well understood: carbon must come predominantly from the triple-alpha reaction of helium, while nitrogen is produced by the conversion of carbon and oxygen that occurs during the CNO cycles of hydrogen burning. However, we lack knowledge of which sites are most important for their generation. In particular, do they come mainly from short-lived massive stars or from longer lived progenitors of asymptotic giant branch (AGB) stars? Coupled with this uncertainty, their production depends on the metallicity of the stars in which the reactions take place.

The sites of carbon synthesis are the type II supernovae, massive stars with wind driven mass loss, and the intermediate- and low-mass stars that die quiescently. The ejecta of core collapse SNe are expected to contribute only a fraction of the present carbon content of the interstellar medium (ISM) (Woosley & Weaver 1995). On the other hand, the carbon – newly synthesized at the He-shell flashes during the TP-AGB phase – can be brought to the

surface by mixing episodes (the so-called third dredge up) and then injected into the ISM by stellar winds (Renzini & Voli 1981). Busso et al. (1999) pointed out “... *while the evolution of massive AGB stars remained a fascinating and open research field, it was gradually recognized that the major role in s-processing and C production had to be played by LMS (low mass stars)*”. These are not fully understood mechanisms, and they may be active in stars of very different masses. Moreover, the run of the $[\text{C}/\text{Fe}]$ ratio with time or metal abundance $[\text{Fe}/\text{H}]$ is presently not well constrained by stellar and galactic evolution models. Much more insight should be gained from observations.

The literature on the origin of carbon has been reviewed by Timmes et al. (1995) and Gustafsson et al. (1999). The former paper concluded that massive star synthesis of primary carbon is sufficient to explain the metal-poor halo dwarf observations, while at $[\text{Fe}/\text{H}] \simeq -0.8$ dex, intermediate- and low-mass stars begin to deposit large amounts of carbon. However, the latter paper states that “*the behavior of C/O ratios as a function of O/H is best explained by the effects of stellar mass loss on massive star yields.*”

Nitrogen is not directly produced in a large amount by hydrostatic He-burning. Nitrogen synthesis requires recycling of material from a region where H-burning occurs through the CNO cycle. Timmes et al. (1995) suggested that no primary nitrogen is produced in the standard massive star models. However, recently, Maeder & Meynet (2000) have shown that a primary nitrogen is produced in

Send offprint requests to: G. Zhao, e-mail: gzhao@bao.ac.cn

^{*} Based on observations carried out at National Astronomical Observatories (Xinglong, China).

rapidly rotating stars within the mass range $10\text{--}15 M_{\odot}$. The nitrogen production for intermediate- and low-mass stars is discussed by Renzini & Voli (1981), van der Hoek & Groenewegen (1997), Marigo et al. (1996, 1998), Busso et al. (1999) and Marigo (2001). Observational data indicate that large amounts of nitrogen are present in the outer layers of evolved stars over a wide mass range. From there, nitrogen can be lost to the ISM through quiescent or violent stellar winds, e.g. in the case of planetary nebulae. Lack of adequate knowledge of the relevant mechanisms prevents accurate predictions of the run of $[N/Fe]$ ratio with metal abundance.

The literature on the origin of nitrogen was reviewed by Henry et al. (2000). Nitrogen has a primary component and a secondary component. At higher abundances the secondary component dominates. Henry et al. (2000) suggested that “*nitrogen is produced mostly (>90%) by intermediate-mass stars, and the relevant stellar masses for production are $4\text{--}8 M_{\odot}$* ”.

As far as the disk stars concerned, many general trends have been discovered during the past decades. The most notable results are correlations of metallicity with age, Galactocentric distance, and vertical distance from the Galactic plane based on photometric, low- and high-resolution observations (e.g. Eggen et al. 1962; Twarog 1980; Edvardsson et al. 1993a; Chen et al. 2000, hereafter Chen00).

For the case of carbon, the particularly important paper is the detailed abundance analysis of 80 F and G dwarfs with $-1.1 < [Fe/H] < +0.25$ by Gustafsson et al. (1999). The main result from their work was the moderate carbon excess in the most metal-poor disk stars. They also suggested that carbon enrichment is by superwinds of metal-rich massive stars.

The present work, based on a differently selected sample of disk stars, aims at exploring and extending the results of Gustafsson et al. (1999). In Sect. 2 we present the observational techniques. The methods of analysis are discussed in Sect. 3. While in Sect. 4 we discuss the possible errors in our results. The relations between abundances, kinematics and ages are given in Sect. 5. And the discussion and conclusions are presented in the last section.

2. Observations

The observational data are taken from Chen00. This sample was observed at National Astronomical Observatories (Xinglong, China) with the Coudé Echelle Spectrograph and a 1024×1024 Tek CCD attached to the 2.16 m telescope, giving a resolution of the order of 40 000. The exposure times were chosen in order to obtain a signal-to-noise ratio of above 150.

The spectra were reduced with standard MIDAS routines for order identification, background subtraction, flat-fielding correction, extraction of echelle orders, wavelength calibration, and continuum fitting (see Chen00 for details). Figure 1 shows a portion of the spectrum of HD 34411A around 7115 Å.

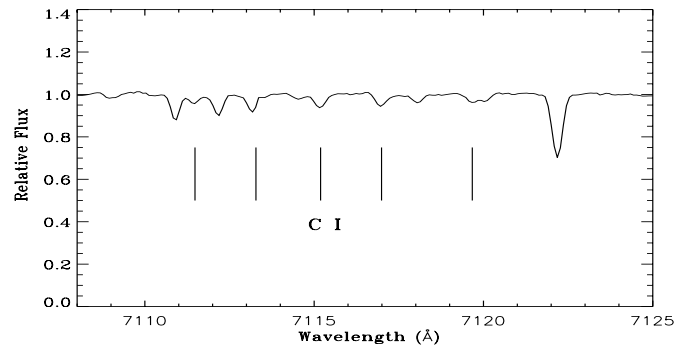


Fig. 1. The C I lines around $\lambda 7115 \text{ \AA}$ in the program star HD 34411A.

3. Analysis

3.1. Model atmospheres

Our analyses are all based on the same type of model, irrespective of temperature, gravity or metal abundance. We use line-blanketed LTE model atmospheres generated and discussed by Fuhrmann et al. (1997). The main characteristics are: the iron opacity was calculated with the improved meteoritic value $\log \epsilon_{Fe} = 7.51$; opacities due to α -elements (O, Ne, Mg, Si, S, Ar, Ca and Ti) for metal-poor stars ($[Fe/H] < -0.6$) were calculated with the α -element abundances enhanced by 0.4 dex; the mixing-length parameter l/H_p was adopted to be 0.5.

3.2. Stellar parameters

The effective temperature in Chen00 was derived from the Strömgren $b-y$ color index using the recent calibration by the infrared-flux method (Alonso et al. 1996). The error in temperature could reach ± 70 K.

Surface gravities in Chen00 were based on Hipparcos parallaxes (ESA 1997). Combining the uncertainties of mass, bolometric correction and temperature, the total error is less than 0.10 dex.

Microturbulence velocities were estimated by requesting that the iron abundance derived from Fe I lines with $\chi > 4$ eV should not depend on equivalent width. The typical error of the microturbulence parameter is about $\pm 0.3 \text{ km s}^{-1}$.

We employ the macroturbulence parameters ζ in the radial-tangential form and adopt values as described in Gray (1984). The projected rotational velocity is obtained as the residual to the observed line profiles, after excluding the known instrumental profiles obtained from the Moon spectra.

3.3. Atomic line data

Collisional broadening through van der Waals interaction with hydrogen atoms is important for strong C I lines (Stürenburg & Holweger 1990; Biémont et al. 1993). The usual procedure is to calculate the interaction

Table 1. Atomic data of C and N lines.

Species	λ [Å]	E_{low} [eV]	E_{up} [eV]	$\log gf$	$\log C_6$
C I	6587.61	8.54	10.42	-1.15	-29.67
C I	7111.48	8.64	10.38	-1.23	-29.68
C I	7113.48	8.65	10.39	-0.85	-29.67
C I	7115.19	8.64	10.38	-1.10	-29.12
C I	7116.99	8.65	10.39	-0.93	-29.12
C I	7119.67	8.64	10.38	-1.15	-29.12
C I	8335.15	7.68	9.17	-0.38	-30.73
[C I]	8727.17	1.26	2.68	-8.17	-32.71
N I	7468.31	10.34	12.00	-0.11	-31.02
N I	8216.34	10.34	11.84	0.15	-31.09
N I	8683.40	10.33	11.76	0.12	-31.13

constants, C_6 , from Unsöld’s approximation corrected by an empirically determined enhancement factor, which is adjusted to make the abundances derived from strong and weak lines agree. Based on considerably improved atomic theory, O’Mara and his collaborators have published damping constants for many neutral transitions (Anstee & O’Mara 1991, 1995; Barklem & O’Mara 1997, 1998; Barklem et al. 1998). In this paper, we adopt their results, although the actual precision of such calculation is still under debate (Leininger et al. 2000). The forbidden [C I] 8727 Å line has not been calculated by O’Mara and his collaborators, and the empirical enhancement factor of 2.5 as suggested by Gustafsson et al. (1999) was used. But this line is not sensitive to damping constant. Comparison with other computations are presented elsewhere (Ryan 1998; Gehren et al. 2001).

Stürenburg & Holweger (1990) and Tomkin et al. (1995) have discussed the gf values of C I lines. The scatter of the individual abundance, caused by oscillator strength error, is the major contributor. In this paper, the oscillator strengths of selected C I and N I lines have been improved from the analysis of corresponding profiles in the Kitt Peak Solar Flux Atlas (Kurucz et al. 1984), with the solar abundance of $\log \varepsilon(\text{C}) = 8.56$ and $\log \varepsilon(\text{N}) = 8.05$ (Anders & Grevesse 1989) respectively. The stellar parameters we adopted in the solar model are: $T_{\text{eff}} = 5780$ K, $\log g = 4.44$ and $\xi = 0.85$. We note that those C I line gf values are similar to the theoretical gf values of Hibbert et al. (1993), for the common C I lines, the average difference $\log gf(\text{solar}) - \log gf(\text{Hibbert})$ is -0.07 ± 0.09 dex; the number after the “ \pm ” here and throughout is standard deviation. Also those gf values are in good agreement with the gf values adopted by Stürenburg & Holweger (1990). Our gf values of three N I lines are nearly the same as the theoretical values of Hibbert et al. (1991), and the difference is very small, less than 0.02 dex. Thus the adoption of theoretical instead of solar oscillator strengths would

not significantly affect the absolute or differential carbon or nitrogen abundances of the program stars (see Table 1).

3.4. Abundance determination

The abundance determinations are made by using the spectral synthesis method. The synthetic spectra are convolved with macroturbulence, rotational and instrumental broadening profiles, in order to match the observed spectral lines. As pointed out by Gustafsson et al. (1999), in most cases, the convolution due to stellar rotation is not necessary for this type stars. The carbon and nitrogen abundances are obtained until a best fit to the observed line profile is provided.

The derived abundances are presented in Table 2. We note that the difference in carbon abundances between the high excitation lines and forbidden line are small, this is in agreement with the results of Carretta et al. (2000). In the spectrum of HD 212029, carbon and nitrogen lines were too weak to allow an accurate measurement of the abundances, thus this star is excluded from further analysis.

4. Error analysis

4.1. Errors in observed spectra and continuum location

For the weak [C I] 8727 Å and N I 8216 Å lines, determining the continuum and fitting the synthetic spectrum to the observed one give the largest errors. These errors vary from star to star depending on the quality of the spectra. For [C I] 8727 Å line, the estimated mean error is ± 0.07 dex for the metal-poor stars, and ± 0.05 dex for the metal-rich stars, while it is larger than 0.1 dex for the weak 8216 Å N I line. This error is nearly negligible for other strong lines.

4.2. Errors in fundamental parameters

The stars in our sample are the same as the stars analyzed in Chen00, where an extensive error analysis is also presented. The error of the effective temperature is estimated in Chen00 to be of the order of 70 K. The logarithm of the gravity has an estimated error less than 0.1 dex. The errors in the model metallicity and in the microturbulence are 0.1 dex and 0.3 km s^{-1} respectively.

The propagation of these parameter errors to the carbon/nitrogen abundance estimation has been investigated by changing the fundamental parameters by a representative amount and then running the synthetic spectrum program to obtain the change in carbon/nitrogen abundance. This is shown in Table 3 for HD 34411A. The statistical errors in the carbon/nitrogen to iron ratio due to uncertainties in the fundamental parameters are around 0.02 and 0.05 dex respectively. The systematic error is about 0.07 dex for carbon, 0.09 dex for nitrogen, which mainly reflects the errors in temperature and surface gravity. The statistical errors in the model metallicity and in the microturbulence are unimportant for the derived

Table 2. Atmospheric parameters and relative abundances for stars from Chen00.

Star HD	T_{eff}	$\log g$	[Fe/H]	ξ	[C/Fe]							[N/Fe]					
					6587	7111	7113	7115	7116	7119	8335	8727	7468	8216	8683	[N/Fe]	
400	6122	4.13	-0.23	1.83			-0.08	-0.09	-0.02			-0.02	-0.05	-0.15		-0.17	-0.16
3454	6056	4.29	-0.59	1.57		-0.08	-0.08				-0.02	0.00	-0.05			0.00	0.00
5750	6223	4.21	-0.44	1.93	0.01		0.05	0.06	0.01		0.06		0.04		-0.05	-0.06	-0.05
6834	6295	4.12	-0.73	1.98	0.28		0.30	0.30	0.32		0.28		0.30				
6840	5860	4.03	-0.45	2.23	0.07		0.06	0.04			0.04		0.05			0.05	0.05
10307	5776	4.13	-0.05	1.80	0.04		0.00	0.03	0.02	0.02	0.00	0.00	0.02	0.05	0.00	0.10	0.05
11007	6027	4.20	-0.16	1.73	0.05		0.03	0.06	0.05	0.06	0.06	0.02	0.05	0.22	0.12	0.22	0.19
11592	6232	4.18	-0.41	2.16	0.00		0.04	0.05	0.09	0.02	0.05	0.06	0.04		0.09	0.10	0.10
19373A	5867	4.01	0.03	1.84	0.07		0.03	0.00	0.00	-0.03	0.07	0.02	0.02		0.05	0.05	0.05
22484	5915	4.03	-0.13	1.97	0.08	0.10	0.06	0.16	0.06	0.08		0.07	0.09		0.00		0.00
24421	5986	4.10	-0.37	1.81			0.06	0.10	0.13			0.13	0.10		0.00	0.00	0.00
25173	5867	4.07	-0.62	1.79	0.25		0.29		0.26	0.24			0.26		0.00	0.00	0.00
25457	6162	4.28	-0.11	2.77	-0.02		-0.04	0.04	0.04	0.06			0.01				
25998	6147	4.35	-0.11	3.24	0.20		0.14	0.16	0.14	0.17			0.16				
33632A	5962	4.30	-0.23	1.56	0.13		0.05	0.14	0.14		0.13	0.14	0.12		0.00	0.00	0.00
34411A	5773	4.02	0.01	1.69	0.04	0.01	0.01	-0.04	-0.04	-0.04	0.04	0.04	0.00	0.08		0.00	0.04
35296A	6015	4.24	-0.14	2.10	0.02		0.00	-0.02	0.02	0.03	0.00		0.01	0.00			0.00
39587	5805	4.29	-0.18	2.16	-0.05		0.00	0.03			0.08		0.02	0.08	0.00		0.04
39833	5767	4.06	0.04	1.88	-0.17		-0.10	-0.18	-0.17		-0.24		-0.17	0.00			0.00
41640	6004	4.37	-0.62	1.98			0.08	0.08			0.10		0.09				
43947	5859	4.23	-0.33	1.73	0.00		0.00	0.03			0.00		0.01				
46317	6216	4.29	-0.24	1.79	0.03		0.05	0.02	0.04	0.02	0.03		0.03	-0.05			-0.05
49732	6260	4.15	-0.70	1.91	0.05		0.05		0.06		0.10		0.07		0.00		0.00
54717	6350	4.26	-0.44	2.00	0.04		0.05	0.05	0.08	0.05	0.03		0.05	0.05	0.03		0.04
55575	5802	4.36	-0.36	1.62	0.08		0.09	0.08			0.09		0.09	0.02	0.00		0.01
58551	6149	4.22	-0.54	2.15	0.00		-0.09	0.02	0.01	-0.02			-0.02				
58855	6286	4.31	-0.31	2.06	-0.05		-0.01	-0.04	-0.02	-0.03	-0.03		-0.03	-0.20	-0.22		-0.21
59380	6280	4.27	-0.17	2.09	0.07		0.06	0.05	0.05	0.04	0.07		0.06		-0.04		-0.04
59984A	5900	4.18	-0.71	1.78							0.22		0.22	0.02			0.02
60319	5867	4.24	-0.85	1.56	0.29		0.32	0.32	0.35		0.30		0.32	0.02	0.05		0.04
62301	5837	4.23	-0.67	1.72	0.33		0.34	0.30	0.32		0.35		0.33		0.05		0.05
63333	6057	4.23	-0.39	1.92			0.08		0.02	0.16			0.09	0.00			0.00
68146A	6227	4.16	-0.09	2.12	0.02			0.00		-0.02	0.01		0.00	0.02			0.02
69897	6243	4.28	-0.28	2.02	-0.04		-0.04	0.00		0.02	-0.06		-0.02	-0.09			-0.09
72945A	6202	4.18	0.00	2.28	-0.03		-0.09	-0.06		-0.04	-0.05		-0.06	-0.03	0.02		0.00
75332	6130	4.32	0.00	2.34	0.05		-0.03	-0.04	-0.03	-0.02	-0.02		-0.02	0.00			0.00
76349A	6004	4.21	-0.49	2.09			0.03				0.05		0.04				
78418A	5625	3.98	-0.26	1.55	0.20		0.23	0.20	0.18		0.30		0.22	0.07			0.07
79028	5874	4.06	-0.05	1.96	0.07		0.09	0.02	0.03	0.02	0.01		0.04	0.05			0.05
80218	6092	4.14	-0.28	1.87	0.18		0.07	0.03	0.07	0.12	0.19		0.11	0.02	0.05		0.04
89125A	6038	4.25	-0.36	1.66	-0.03		-0.10	-0.11			-0.03		-0.07	-0.09			-0.09
90839A	6051	4.36	-0.18	2.14	0.06		0.03	0.04	-0.01	-0.02	0.03		0.01	0.07	0.05		0.06
91889A	6020	4.15	-0.24	1.66	-0.08		-0.14	-0.07	-0.06		-0.07		-0.08		-0.12		-0.12
94280	6063	4.10	0.06	2.00	-0.03		-0.02	-0.02	-0.04	-0.06			-0.03		-0.15		-0.15
95128	5731	4.16	-0.12	1.87	0.17		0.16	0.16	0.12		0.19		0.16	-0.08	-0.05		-0.06
97916	6445	4.16	-0.94	2.11			-0.08				0.00		-0.04				

carbon/nitrogen abundance (Andersson & Edvardsson 1994; Gustafsson et al. 1999, and references therein).

We have also searched for correlations between carbon/nitrogen abundances and atmospheric parameters. There is no correlation of [C/Fe] and [N/Fe] with either T_{eff} or $\log g$. The weak correlation between [C/Fe] and microturbulence parameter found by Andersson & Edvardsson (1994) is not confirmed in this work.

We estimate that the total random error is 0.1 dex in the carbon abundance, 0.2 dex in the nitrogen abundance.

4.3. Errors due to departures from LTE

Statistical equilibrium calculations for the carbon features have been carried out by Stürenburg & Holweger (1990) and Tomkin et al. (1992, 1995). These

Table 2. continued.

Star HD	T_{eff}	$\log g$	[Fe/H]	ξ	[C/Fe]								[N/Fe]			
					6587	7111	7113	7115	7116	7119	8335	8727	$\overline{\text{[C/Fe]}}$	7468	8216	8683
100180A	5866.	4.12	-0.11	1.87	0.05	0.06	0.03	0.00	0.00	0.03	0.06		0.03	0.15		0.15
100446	5967.	4.29	-0.48	1.86	0.12		0.12	0.13	0.16		0.10		0.12	0.15		0.15
100563	6423.	4.31	-0.02	2.63	0.20	0.20	0.12	0.12		0.16	0.17		0.16	-0.02	0.02	0.00
101676	6102.	4.09	-0.47	1.96		0.10	0.07	0.07	0.06		0.10		0.08	0.15	0.15	0.15
106516A	6135.	4.34	-0.71	1.48		0.43	0.38	0.41	0.41	0.39	0.45		0.41	0.48	0.38	0.43
108510	5929.	4.31	-0.06	2.00	0.03	0.02	0.01	0.01	-0.04	0.11	0.11		0.04	-0.42	-0.40	-0.41
109303	5905.	4.10	-0.61	1.69	0.29	0.24	0.26	0.20	0.16	0.18	0.20		0.22			
114710	5877.	4.24	-0.05	1.77	0.03		-0.02	-0.02	-0.03	-0.02	0.03		0.01	-0.15	-0.18	-0.17
115383A	5866.	4.03	0.00	2.09			0.05	0.01		0.02	0.00		0.02	0.07		0.07
118244	6234.	4.13	-0.55	2.29			0.05	0.09	0.03	0.06	0.04		0.05	0.00		0.00
121560	6059.	4.35	-0.38	1.69	-0.10		-0.09	-0.10			-0.07		-0.09		0.00	0.00
124244	5853.	4.11	0.05	1.92	-0.02		-0.02	0.05		-0.07	-0.05		-0.04	-0.15		-0.15
128385	6041.	4.12	-0.33	2.07			0.00		-0.05	0.02	0.04		0.0	-0.20	-0.10	-0.15
130948	5780.	4.18	-0.20	2.15	-0.01		0.02	0.02	0.05		0.03		0.02	0.00	0.04	0.02
132254	6231.	4.22	0.07	2.05	-0.16		-0.12	-0.14	-0.10		-0.15		-0.13	-0.09	-0.15	-0.12
139457	5941.	4.06	-0.52	1.95	0.24		0.22	0.18	0.20		0.16		0.20		0.00	0.00
142373	5920.	4.27	-0.39	1.48	-0.02		0.00	0.02					-0.01		0.00	0.00
142860A	6227.	4.18	-0.22	2.15	-0.05	-0.03	-0.03	-0.03	-0.05	-0.05	-0.07		-0.04	0.00	-0.02	-0.01
146099A	5941.	4.10	-0.61	1.79	0.08						0.14		0.11	0.02		0.02
149750	5792.	4.17	0.08	1.96			0.08	0.09	0.06	0.07			0.08			
154417	5925.	4.30	-0.04	1.78			0.09	0.12	0.08		0.15		0.11	0.08	0.06	0.07
157347	5654.	4.36	-0.02	1.89	-0.12		-0.10	-0.09	-0.12	-0.10	-0.08	-0.05	-0.09		-0.29	-0.29
157466	5935.	4.32	-0.44	1.89	-0.10		-0.08	-0.04			-0.08	-0.12	-0.08		0.08	0.00
162004B	6059.	4.12	-0.08	2.34	0.00		-0.04	-0.03	0.00		-0.02	0.03	-0.01		-0.06	-0.06
167588	5894.	4.13	-0.33	1.72	0.15		0.07		0.09		0.07	0.09		-0.04	-0.06	-0.05
168009	5719.	4.08	-0.07	1.82			0.25	0.19	0.25	0.24		0.13	0.21	0.12		0.06
170153A	6034.	4.28	-0.65	2.36	0.38		0.43	0.37	0.35		0.40		0.39	0.00		-0.03
184601	5830.	4.20	-0.81	1.50	0.33		0.37	0.35	0.39	0.40		0.35	0.37		0.15	0.21
189340	5888.	4.26	-0.19	2.28	0.05						-0.05	-0.02	-0.01			-0.05
191862A	6328.	4.19	-0.27	2.88					-0.02	-0.05	-0.10	-0.04	-0.05	-0.40		-0.49
198390	6339.	4.20	-0.31	1.92							0.19	0.20	0.20			
200580	5829.	4.39	-0.58	1.66			0.32						0.32			
201891	5827.	4.43	-1.04	1.55				0.38	0.41		0.32		0.37			
204306	5896.	4.09	-0.65	1.70	0.20		0.22		0.26			0.15	0.21		0.07	0.06
204363	6141.	4.18	-0.49	2.06	0.20			0.13	0.10			0.15	0.15		0.15	0.15
206301	5682.	3.98	-0.04	2.12			-0.09	-0.09	-0.11		-0.07	-0.10	0.09	-0.04	0.00	-0.02
206860	5798.	4.25	-0.20	2.33			-0.08	-0.03	-0.01		0.00	0.00	-0.02	0.12	0.10	0.11
208906A	5929.	4.39	-0.73	1.47			0.26	0.24		0.23	0.28	0.24	0.25			0.05
209942A	6022.	4.25	-0.29	2.26			0.11	0.08	0.15	0.08		0.12	0.11	0.06	0.05	0.08
210027A	6496.	4.25	-0.17	1.97			0.00	-0.01	0.03	-0.03	0.00	-0.03	-0.01	-0.06		-0.08
210752	5847.	4.33	-0.68	2.39			0.16				0.15	0.16	0.16		0.00	0.00
212029A	5875.	4.36	-1.01	2.03												
215257	5976.	4.36	-0.65	1.74								0.06	0.06			
219623A	6039.	4.07	0.02	1.84			0.12	0.04	0.08			0.04	0.07	0.00	0.02	-0.01

calculations indicate that non-LTE abundance corrections are small (<0.1 dex) for lines near $\lambda 7100 \text{ \AA}$ and the line $\lambda 8385 \text{ \AA}$. Gustafsson et al. (1999) have already discussed that the non-LTE correction is negligible for the forbidden [C I] $\lambda 8727 \text{ \AA}$ line.

Takeda (1994) discussed the non-LTE effects of nitrogen for the Sun and Procyon. He found that the non-LTE effects in the Sun and Procyon are small, less than 0.1 dex, for most NI lines. Rentzsch-Holm (1996) also found that the non-LTE correction (NLTE-LTE) in the Sun is typically -0.05 dex.

Our program stars are not greatly different from the Sun and Procyon, so the non-LTE correction of carbon/nitrogen abundances is not affected significantly.

4.4. Comparison with other results

4.4.1. Carbon

Carbon abundances of the disk stars have been determined by several groups. We have 8 stars in common with Gustafsson et al. (1999) and 12 stars with Tomkin et al. (1995). The average differences between our [C/Fe]

Table 3. Dependence of C and N abundances on the estimated systematic errors in effective temperature, gravity and micro-turbulence for the program star HD 34411A.

Change	[C/Fe]								[N/Fe]		
	6587 Å	7111 Å	7113 Å	7115 Å	7116 Å	7119 Å	8335 Å	8727 Å	7468 Å	8216 Å	8683 Å
$\Delta T_{\text{eff}} = +70$ K	-0.03	-0.02	-0.02	-0.05	-0.04	-0.02	-0.05	-0.03	-0.06	-0.07	-0.06
$\Delta \log g = +0.1$	+0.04	+0.03	+0.03	+0.03	+0.03	+0.03	+0.04	+0.03	+0.04	+0.03	+0.04
$\Delta \xi = +0.3$	0.00	0.00	0.00	0.00	0.00	0.00	0.00	-0.02	0.00	0.00	0.00

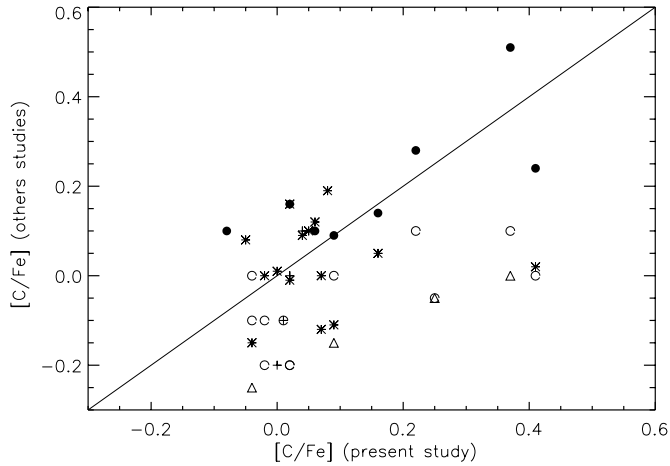


Fig. 2. Comparison of derived [C/Fe] for stars in common with other studies. Plusses (+) are from Clegg et al. (1981); open circles (o) are from Larid (1985); asterisks (*) are from Tomkin et al. (1995); filled circles (•) are from Gustafsson et al. (1999).

and theirs are -0.05 ± 0.11 and 0.04 ± 0.14 , respectively. The agreement is quite satisfactory. Furthermore, we have 15 stars in common with Larid (1985) and 4 stars with Carbon et al. (1987). The differences in [C/Fe] are large with deviations of 0.17 ± 0.12 and 0.28 ± 0.07 , respectively. Notice the fact that we use high-excitation lines of high-resolution spectra, while they used CH molecular lines of low-resolution spectra. It seems there is a systematic difference between abundances derived from CH lines and C I lines. This argument is weakened, however, by the large discrepancy of the stellar parameters adopted by them and us. A comparison between this and other work is shown in Fig. 2.

4.4.2. Nitrogen

Based on the high-resolution spectra, Clegg et al. (1981) determined nitrogen abundances from NI and CN lines (near 8050 Å) for some disk stars. Laird (1985) derived nitrogen abundances in 116 dwarfs using intermediate-resolution spectra from the 3360 Å band of molecular NH. Carbon et al. (1987) determined nitrogen abundances for 83 dwarfs using the low-resolution, moderate signal to noise ratio ($S/N \sim 50$) spectra from the NH molecular band near 3360 Å.

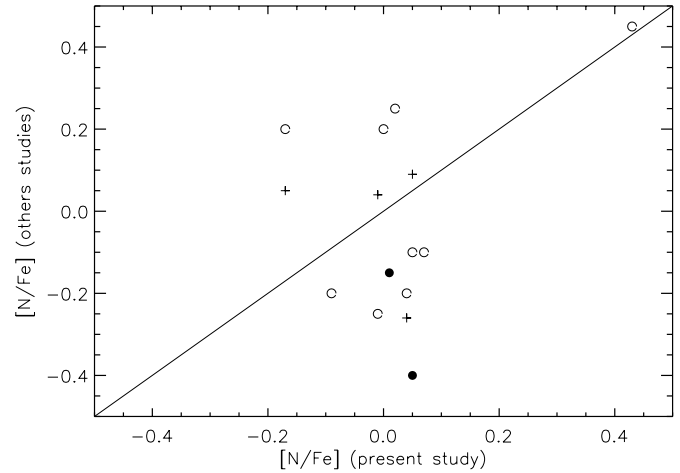


Fig. 3. Comparison of derived [N/Fe] for the stars in common with other studies. Plusses (+) are from Clegg et al. (1981); open circles (o) are from Larid (1985); filled circles (•) are from Carbon et al. (1987).

We have 4 stars in common with Clegg et al. (1981) and 8 stars with Larid et al. (1985). Although the systematic deviation of [N/Fe] is small, 0.01 ± 0.22 and 0.00 ± 0.22 respectively, the rms is very large, reflecting the difficulties in the determination of nitrogen abundances. The comparison of this work with others is plotted in Fig. 3.

5. Relations between abundances, kinematics and ages

In this section we describe our results by detailing the correlations of abundances, stellar ages and stellar kinematics. We divide our program stars into three groups as in Chen00: group A, metal-poor ($[\text{Fe}/\text{H}] < -0.5$) with positive V_{LSR} ; group C, metal-poor ($[\text{Fe}/\text{H}] < -0.5$) with $V_{\text{LSR}} < -50 \text{ km s}^{-1}$ and group B are the remaining stars. Note that HD 97916 is a typical halo star as already discussed in Chen00.

5.1. Relations between abundances

The plot of [C/Fe] against [Fe/H] shown in Fig. 4a confirms the enrichment of carbon relative to iron for the most metal-poor disk stars found in previous investigations (Friel & Boesgaard 1992;

Andersson & Edvardsson 1994; Tomkin et al. 1995; Gustafsson et al. 1999). For our group C stars, the $[C/Fe]$ is around 0.3 dex, while $[C/Fe]$ is flat for $[Fe/H] > -0.4$. A striking feature of the plot is that the transition from $[C/Fe] \sim 0.0$ to $[C/Fe] \sim +0.4$ for group A stars is made over a small range in $[Fe/H]$ or rather abruptly at $[Fe/H] \simeq -0.7$. There are also some group C and A stars in Tomkin et al. (1995, in Fig. 8) and the same trend can be found in their sample, as well as the same decreasing trend for the metal-poor part of group B stars. We note, however, that Gustafsson et al. (1999) did not find this trend, which may be due to the small number of group A stars in their sample or different lines used to determine the carbon abundances. In short, there seems to be an abrupt drop of $[C/Fe]$ at $[Fe/H] \simeq -0.7$. Two scenarios may explain this result: one is that it may indicate the large contribution of iron from type Ia SNe at that time; another is that when the metallicity is relatively higher, the mass loss rate is more important, the star enters the WC phase at an earlier stage, thus less helium has been changed into carbon (Maeder & Meynet 1993). Portinari et al. (1998) also pointed out that, *for massive stars* ($9 M_{\odot} < M < 120 M_{\odot}$), *carbon yields decrease again moving from the $Z = 0.008$ to the $Z = 0.05$, both because a higher mass loss rate is able to take more helium away before it turned to carbon, and because with an increasing metallicity an increasing fraction of the original carbon is turned to ^{14}N in the CNO cycle*, while Prantzos et al. (1994), Gustafsson et al. (1999) and Henry et al. (2000) suggested that carbon production could be favoured at higher metallicities, in order to explain the observed correlation between C/O and O/H.

The decrease of $[C/Fe]$ with increasing $[Fe/H]$ in the galactic disk is very different from the variation of the s-element abundances with $[Fe/H]$. Using the standard infall Galactic chemical evolution (hereafter GCE) models and yields of Maeder (1992) or Portinari et al. (1998), Liang et al. (2001) found that $[C/Fe]$ increases from $[Fe/H] \sim -1$ to $[Fe/H] \sim -0.5$, which was in contradiction with the observations (see also Portinari et al. 1998). In addition, $[C/Fe]$ was above the observations in the metal-rich region. Prantzos et al. (1994) also studied the formation of oxygen and carbon in the Galaxy and found that, if the duration of the halo phase was on the order 1–2 Gyrs as is currently believed, intermediate- or low-mass stars should not have been the main carbon sources. As noted already by Gustafsson & Ryde (2000), however, the GCE model calculations of Prantzos et al. (1994), with contributions added also from the intermediate- and low-mass stars according to Renzini & Voli (1981), fit the recent observation results (Tomkin et al. 1995; Gustafsson et al. 1999 and this work) rather well, although the C/O ratios of comparatively metal-rich halo stars become too high. In that model, a significant amount of the carbon in the disk stars was contributed by intermediate- and low-mass stars. If low-mass stars produce significant amounts of carbon as reviewed by Busso et al. (1999), the discrepancy for the metal-rich halo stars would diminish,

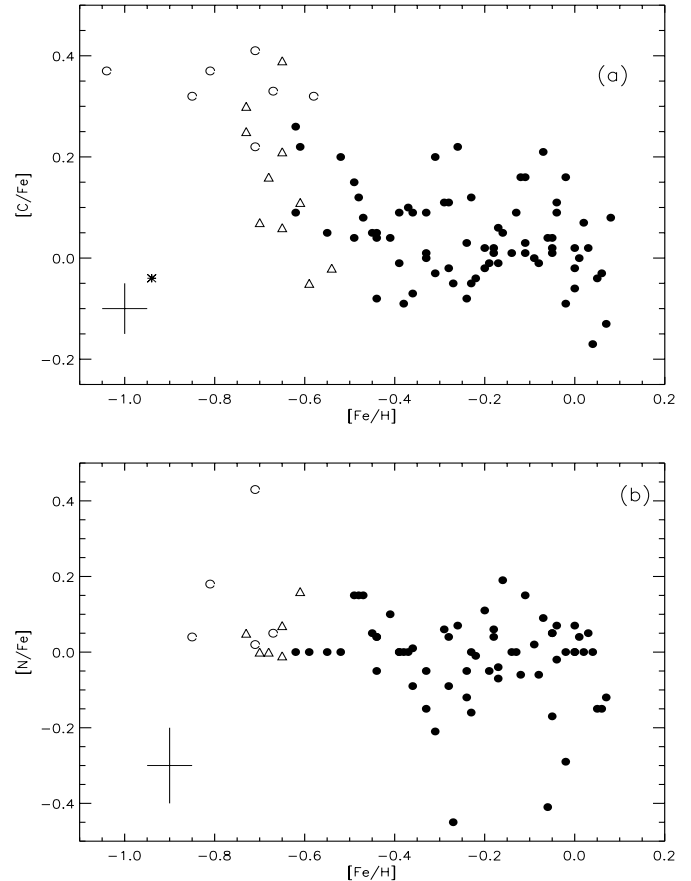


Fig. 4. Abundance patterns for $[C/Fe]$ and $[N/Fe]$ with three groups of stars: open triangles (Δ): group A; filled circles (\bullet): group B; open circles (\circ): group C and asterisk ($*$): halo star HD 97916.

but they may produce too much carbon at late stages. This conflict could possibly be resolved by advocating more efficient carbon production by low-mass metal-poor stars, as Marigo (2001) suggested that, *for intermediate- and low-mass stars, the carbon yields are larger at low metallicities, both because the third dredge-up and hot-bottom burning are more efficient, and because TP-AGB lifetimes are longer*.

The spread of $[C/Fe]$ at $[Fe/H] \simeq -0.7$ is rather large. Does it reflect the intrinsic scatter of the stellar $[C/Fe]$ ratios or can it, alternatively, be attributed to observational error? Additional observations will be needed to examine the intriguing patterns. In addition, the $[C/Fe]$ ratio of the halo star HD 97916 is nearly solar, this result is in agreement with other halo stars investigated by Tomkin et al. (1992).

Relative abundances of $[N/Fe]$ as a function of $[Fe/H]$ are shown in Fig. 4b. The result generally confirms the published trend based on lower quality spectroscopic analysis (Larid 1985; Carbon et al. 1987). However, there is a N-rich metal-poor star HD 106516 A, which was found by Larid (1985) and this type of star was discussed in detail by Beveridge & Sneden (1994). The three metal-rich stars, namely HD 108510, HD 157347 and HD 191862A, show unexpectedly low nitrogen abundances ($[N/Fe] < -0.3$).

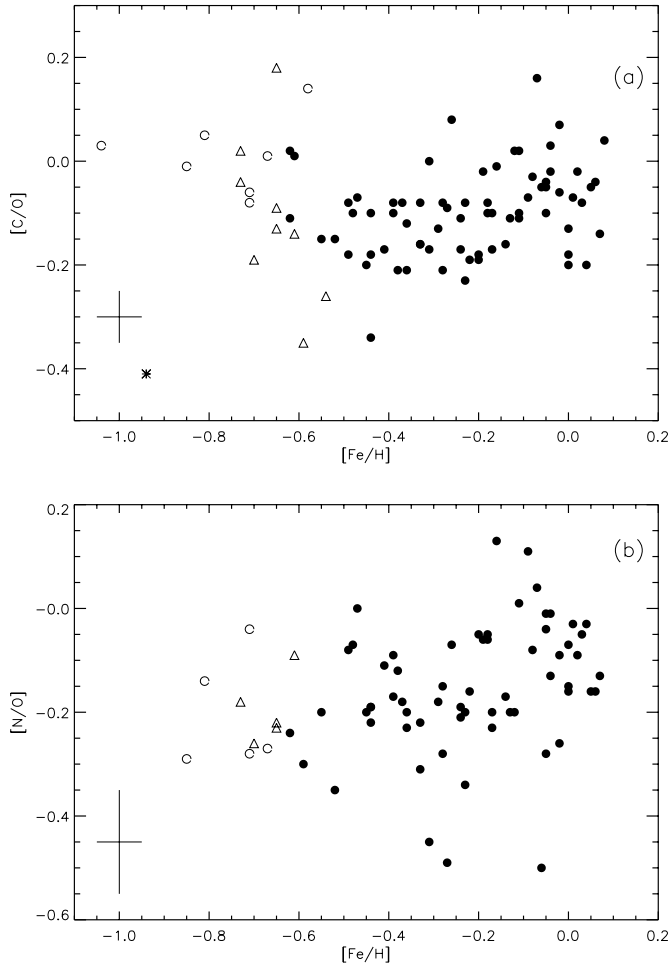


Fig. 5. Relations of [C/O] and [N/O] vs. [Fe/H]. Symbols are same as Fig. 4.

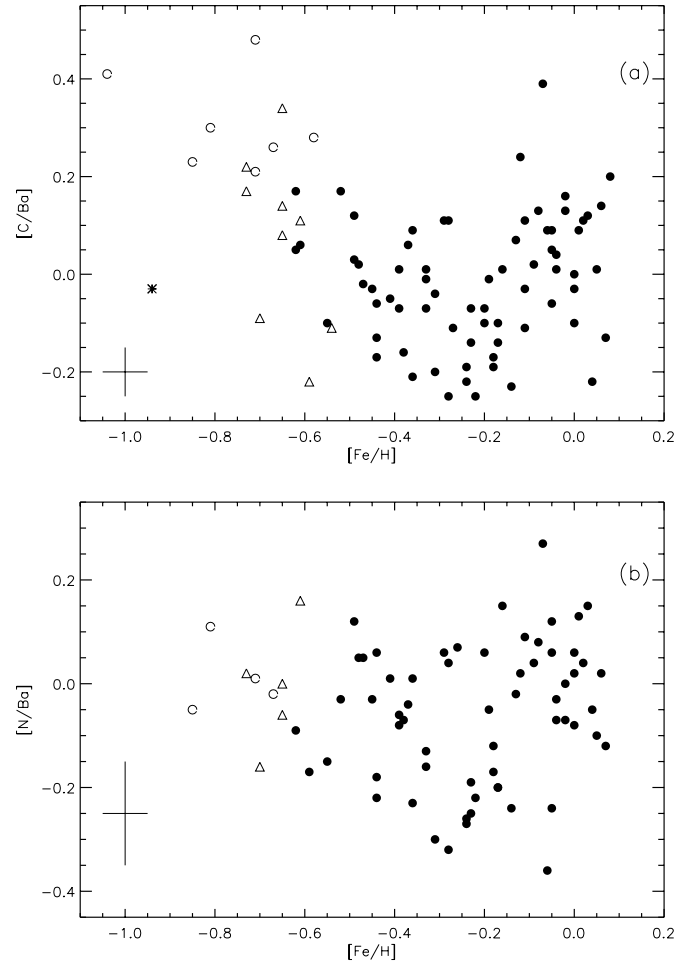


Fig. 6. Relations of [C/Ba] and [N/Ba] vs. [Fe/H]. Symbols are same as Fig. 4.

They are interesting because none of the present scenarios can explain their low nitrogen abundances, and the previous discovery of these low nitrogen abundance focus on the metal-poor stars as shown in Clegg (1977). The behavior of other elements and kinematics for the three stars is not special.

The ratios of heavy elements are expected to reveal the characteristics of stellar yields. Massive stars ($8 M_{\odot} < M < 40 M_{\odot}$), which become type II SNe, are responsible for the nucleosynthesis of oxygen and part of iron in disk stars (Timmes et al. 1995), while the less massive AGB stars are thought to be the primary source of barium. The masses of AGB stars run up to about $8 M_{\odot}$, but it is probably the lower mass (about $1-3 M_{\odot}$) and longer-lived stars that dominate the synthesis of elements like barium (Busso et al. 1999).

There are two features that can be found in Figs. 5a and 6a. Firstly, the large spread of [C/O] or [C/Ba] around $[\text{Fe}/\text{H}] \simeq -0.7$ is evident. As oxygen is produced mainly by massive stars, the steep slope of [C/O] may reflect the fact that less carbon is ejected from high metallicity massive stars (Maeder & Meynet 1993; Portinari et al. 1998), while

the decrease of [C/Ba] could be due to large barium contribution from low-mass stars. Secondly, there is a slight increase in [C/O] or [C/Ba] with increasing metallicity for $-0.4 < [\text{Fe}/\text{H}] < +0.2$, this behavior could be explained by the large contribution of carbon, but no (or a slight) contribution of oxygen from low-mass stars, which is in agreement with the model calculations by Marigo et al. (1996, 1998), Forestini & Charbonnel (1997), Busso et al. (1999) and Marigo (2001); or could instead be explained by the increase of carbon yields from massive stars with metallicity, as suggested by Gustafsson et al. (1999). We note, however, that, although the model calculations of Gustafsson et al. (1999) were in general agreement with the observed relations for [C/O] vs. [Fe/H], the fit is not perfect. For example, for [C/O] a value is predicted of about -0.4 at $[\text{Fe}/\text{H}] \sim -0.6$, this is not seen in their observations. Alternatively, the increase in [C/Ba] may be due to the decrease of barium abundances for more metal-rich stars (Chen00). In addition, there seems to be a tendency for the halo stars to have low [C/O] ratios as compared with disk stars (McWilliam 1997; Gustafsson et al. 1999); this is the case for our halo star HD 97916.

Excluding the low nitrogen abundance stars, a gradual increase of $[N/O]$ ratio with $[Fe/H]$ can be found in Fig. 5b, reflecting the difference in time scale between oxygen and nitrogen producing stars. Oxygen is expected to be produced predominantly in the SN II explosion of short lived massive stars, while nitrogen is probably produced by intermediate-mass stars, as suggested by Timmes et al. (1995), Portinari et al. (1998) and Liang et al. (2001). Recently, Marigo (2001) have shown that the nitrogen produced by intermediate-mass stars with hot-bottom burning is of primary origin and that nitrogen production is favoured at lower metallicities. Liang et al. (2001) found that the primary nitrogen from intermediate-mass stars plays an important (possibly dominant) role in the nitrogen production (their Fig. 8b).

Although there is a large scatter, the $[N/Ba]$ is about solar through the whole metallicity region explored in this paper (Fig. 6b), which may be explained by the common sources of nitrogen and barium. This suggestion is further supported by the N-rich stars, which are also rich in *s*-process elements (Beveridge & Sneden 1994). However, this argument is weakened by the possibility that the barium is favorably produced by intermediate metallicity low-mass stars (Busso et al. 1999).

5.2. Stellar kinematics as function of metallicity

As discussed in Edvardsson et al. (1993b), and Chen00, there is a tight correlation between V_{LSR} and the mean Galactocentric distance in the stellar orbit, R_m . Hence, when the velocity component in the direction of Galactic rotation, V_{LSR} is investigated as a function of metallicity, we can trace $[C/Fe]$ and $[N/Fe]$ ratios at different Galactocentric distances assuming that R_m is a reasonable estimator of the radius of the original orbit. In Figs. 7a and 7b, we present the V_{LSR} vs. $[C/Fe]$ and $[N/Fe]$ respectively. There is a rough correlation between kinematic parameters and their carbon abundances in the disk stars. Note that our group C stars (Fig. 7a) have lower V_{LSR} , smaller R_m , and higher carbon abundances. Considering that they are old, the intermediate- and low-mass stars have no time to contribute significant carbon. The carbon has probably come from the superwinds of massive stars, while a large spread of $[C/Fe]$ can be found for our group A stars with large Galactocentric distance. These results may indicate a radial abundance gradient in the disk, implying a slower evolution in the outer disk than the inner. This is compatible with a low SFR, due to the lower gas density in the outer disk (Chen00).

Generally, no correlation between nitrogen abundances and kinematics can be found in our samples (Fig. 7b).

5.3. Age-metallicity relation in the disk

Chen00 have determined individual age for these stars. In Fig. 8 we show carbon and nitrogen abundances plotted against the stellar ages from Chen00. The striking

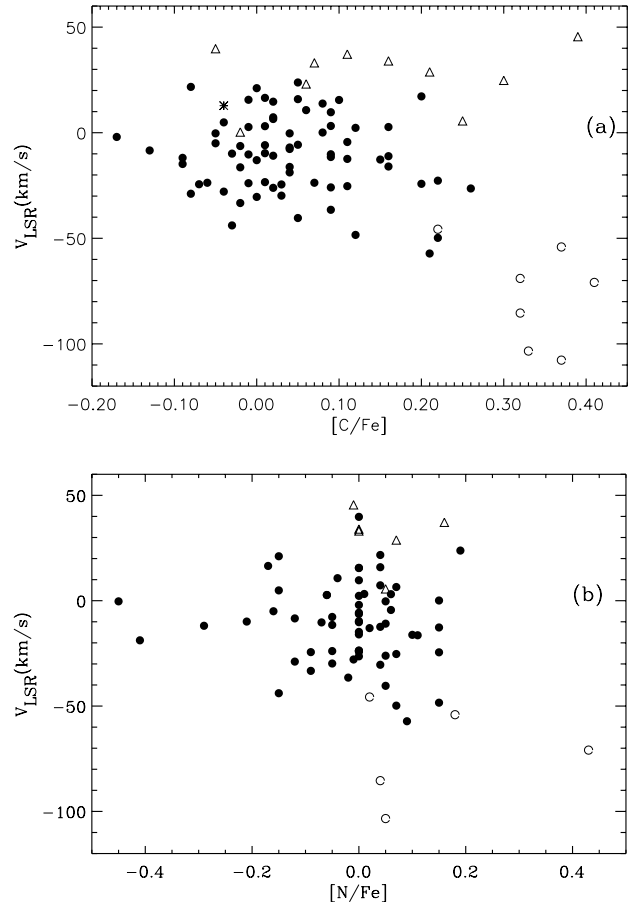


Fig. 7. Rotation velocity vs. $[C/Fe]$ and $[N/Fe]$. Symbols are same as Fig. 4.

feature of the plot is that, for stars within a given range of Galactocentric distance, the increase of the carbon abundance with decreasing stellar age is either marginal or non-existent. A similarly great scatter is found in the $[C/H]$ – age diagram (Gustafsson et al. 1999) and in the $[Fe/H]$ – age diagram (Edvardsson et al. 1993a; Chen00). This may indicate a cosmic spread in $[C/Fe]$ at a given age. It seems that $[C/H]$ is more tightly related to metallicity than to age. However, there is a possibility that the spread in the $[C/H]$ and $[N/H]$ – age relation is due to the diffusion of stars formed at different distances from the Galactic center into orbits close to the solar circle (Edvardsson et al. 1993a; Wielen et al. 1996; Gustafsson et al. 1999).

Unexpectedly, carbon abundances of group A stars with larger galactocentric distances slightly decrease with decreasing age. Tomkin et al. (1995) found the same result, and suggested “*it is a surprising possibility.*” A large sample of these type stars is needed to confirm this trend.

6. Discussion and conclusions

We have determined carbon and nitrogen abundances for 90 Galactic disk stars, spanning the range $-1.0 < [Fe/H] < +0.2$. We confirm the moderate enrichment of carbon relative to iron for the most metal-poor disk stars, and we find that $[C/Fe]$ decrease abruptly

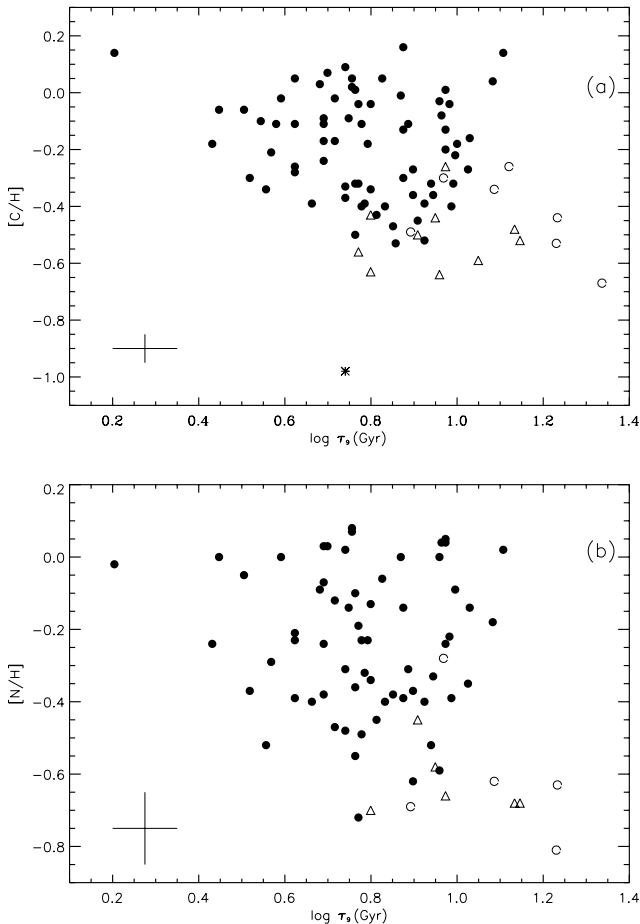


Fig. 8. Relation of [C/H] and [N/H] vs. age. Symbols are same as Fig. 4.

at $[\text{Fe}/\text{H}] \simeq -0.7$, while the observed behavior of $[\text{N}/\text{Fe}]$ is nearly solar in the disk stars. Based on these results, we briefly discussed the sources of carbon and nitrogen.

Wheeler et al. (1989) reviewed carbon abundances and concluded that $[\text{C}/\text{Fe}] \sim 0.0$ independent of $[\text{Fe}/\text{H}]$ but with a possible increase in $[\text{C}/\text{Fe}]$ below $[\text{Fe}/\text{H}] \sim -1.5$. Recent studies of carbon abundance indicate that $[\text{C}/\text{Fe}]$ is enhanced with declining $[\text{Fe}/\text{H}]$ in the Galactic disk (e.g. Fried & Boesgaard 1992; Andersson & Edvardsson 1994; Tomkin et al. 1995; Gustafsson et al. 1999; and this work). Thus, in the disk $[\text{C}/\text{Fe}]$ and $[\alpha/\text{Fe}]$ show morphologically similar trends with $[\text{Fe}/\text{H}]$.

The threshold temperature of He burning and production of ^{12}C via the triple alpha process is $\sim 10^8$ K, a temperature that is reached in both massive ($M > 8 M_{\odot}$) and intermediate-mass ($1 < M < 8 M_{\odot}$) stars. The main nucleosynthesis site of carbon has been argued for many years. Some authors suggested that the main sources of carbon are intermediate- and low-mass stars (Wheeler et al. 1989; Timmes et al. 1995; Chiappini et al. 1997; Kobulnicky & Skillman 1998; Oberhummer et al. 2000). Others suggested that the massive stars with wind driven mass loss could be the main carbon source during the whole Galactic evolution (Prantzos et al. 1994;

Gustafsson et al. 1999; Karlsson et al. 1998; Henry et al. 2000; Carigi 2000), while, some authors argued that the carbon sources are still not clear (Garnett et al. 1999; Gustafsson & Ryde 2000; Hou et al. 2000; Liang et al. 2001). Our observational results show that high carbon abundances are found for group C stars. Considering their old ages, intermediate- and low-mass stars have no time to contribute significant amounts of carbon. More probably it comes from metal-rich Wolf-Rayet stars, which eject a significant amount of carbon into the ISM by radiative-driven stellar wind at the early time of the disk evolution (Maeder 1992). Moreover, the steep decrease of $[\text{C}/\text{O}]$ at $[\text{Fe}/\text{H}] \simeq -0.7$ could indicate that less carbon is ejected by massive stars at this metallicity (Maeder & Meynet 1993; Portinari et al. 1998). The increase of $[\text{C}/\text{O}]$ or $[\text{C}/\text{Ba}]$ with increasing $[\text{Fe}/\text{H}]$ for $-0.4 < [\text{Fe}/\text{H}] < +0.2$ could be due to the increase of carbon yields from massive stars with metallicity, as already suggested by Gustafsson et al. (1999); or could instead be due to a large carbon contribution from low mass stars.

Although carbon abundances of the most metal-poor disk stars may resemble the α element pattern, the abundance trends are quite different and uncertain. It is clear that further study is required to understand $[\text{C}/\text{Fe}]$ as a function of $[\text{Fe}/\text{H}]$.

Nitrogen abundances have been obtained by Clegg et al. (1981), Tomkin & Lambert (1984), Laird (1985) and Carbon et al. (1987) with the result that $[\text{N}/\text{Fe}]$ is essentially solar, irrespective of the metal content of the star, but with considerable scatter. Our preliminary analysis confirms previous results that $[\text{N}/\text{Fe}]$ is nearly constant in a wide range of $[\text{Fe}/\text{H}]$.

Like carbon, nitrogen production via the CNO cycles may occur in either massive or intermediate mass stars. However, discovering the origin of nitrogen is further complicated by the fact that the seed carbon needed for its production may either have been present when the star was born or is synthesized within the star during its lifetime. The main nucleosynthesis site of nitrogen was discussed by Vila-Costas & Edmunds (1993), Timmes et al. (1995), Henry et al. (2000), and Liang et al. (2001), they suggest that nitrogen is produced principally in intermediate-mass stars of $4 \sim 8 M_{\odot}$. A gradual increase of $[\text{N}/\text{O}]$ with $[\text{Fe}/\text{H}]$ for the disk stars found in this work may confirm this suggestion. The primary nitrogen from intermediate-mass stars may also play an important role in the nitrogen production.

Combined with models of galactic chemical evolution, our results allow us to throw some light on the Galaxy evolution. As already discussed by Chen00, group C stars are most like thick disk stars (very old, metal-poor and low V_{LSR}), for which Fuhrmann (1998, 2000) found a similar $[\text{Mg}/\text{Fe}]$ to the halo stars, however, the behavior of $[\text{C}/\text{Fe}]$ is quite different between the thick disk and the halo stars at the same $[\text{Fe}/\text{H}]$. This result favors the suggestion that the halo and thick disk have their own distinct evolution paths (Gilmore 1995; Fuhrmann 2000).

In order to confirm the present results for carbon and nitrogen, it is necessary to investigate a large sample of stars with various metallicities, especially for the metal-poor stars of the thick disk and the halo, which will be an important step in improving our present understanding of stellar nucleosynthesis and the chemical evolution of the Galaxy.

Acknowledgements. We are very grateful to Prof. Thomas Gehren for his valuable comments and many stimulating discussions. The authors are grateful to Dr. Johannes Reetz for providing the code SIU for synthetic spectrum computations. We are thankful for the suggestions of an anonymous referee that much improved the final version of this paper. This research was supported by the National Natural Science Foundation of China under the grant No. 19725312 and NKBRSF 1999075406.

References

- Andres, E., & Grevesse, N. 1989, *Geochim. Cosmochim. Acta*, 53, 197
- Andersson, H., & Edvardsson, D. 1994, *A&A*, 290, 590
- Anstee, S. D., & O'Mara, B. J. 1991, *MNRAS*, 253, 549
- Anstee, S. D., & O'Mara, B. J. 1995, *MNRAS*, 276, 859
- Barklem, P. S., & O'Mara, B. J. 1997, *MNRAS*, 290, 102
- Barklem, P. S., & O'Mara, B. J. 1998, *MNRAS*, 300, 863
- Barklem, P. S., O'Mara, B. J., & Ross, J. E. 1998, *MNRAS*, 296, 1057
- Beveridge, C. R., & Sneden, C. 1994, *AJ*, 108, 285
- Biémont, E., Hibbert, A., Godefroid, M., & Vaeck, N. 1993, *ApJ*, 412, 431
- Boothroyd, A. I., & Sackmann, I.-J. 1988, *ApJ*, 416, 762
- Busso, M., Gallino, R., & Wasserburg, G. J. 1999, *ARA&A*, 37, 239
- Carbon, D. F., Barbuy, B., Kraft, R. P., Friel, E. D., & Suntzeff, N. B. 1987, *PASP*, 99, 335
- Carigi, L. 2000, *Rev. Mex. Astron. Astrofis.*, 36, 171
- Carretta, E., Gratton, R. G., & Sneden, C. 2000, *A&A*, 356, 238
- Chen, Y. Q., Nissen, P. E., Zhao, G., Zhang, H. W., & Benon, T. 2000, *A&AS*, 141, 491 (Chen00)
- Chiappini, C., Matteucci, F., & Gratton, R. 1997, *ApJ*, 477, 765
- Clegg, R. E. S. 1977, *MNRAS*, 181, 1
- Clegg, R. E. S., Lambert, D. L., & Tomkin, J. 1981, *ApJ*, 250, 262
- Edvardsson, B., Andersen, J., Gustafsson, B., et al. 1993a, *A&A*, 275, 101
- Edvardsson, B., Gustafsson, B., Nissen, P. E., et al. 1993b, in *Panchromatic view of Galaxies*, ed. G. Hensler, Ch. Thesis, & J. Gallagher, 401
- EGEN, O. J., Lynden-Bell, D., & Sandage, A. R. 1962, *ApJ*, 136, 748
- ESA 1997, *The Hipparcos and Tycho Catalogues*, ESA, SP-1200
- Forestini, M., & Charbonnel, C. 1997, *A&AS*, 123, 241
- François, P., & Matteucci, F. 1993, *A&A*, 280, 136
- Friel, E. D., & Boesgaard, A. M. 1990, *ApJ*, 351, 480
- Friel, E. D., & Boesgaard, A. M. 1992, *ApJ*, 387, 170
- Fuhrmann, K. 1998, *A&A*, 338, 161
- Fuhrmann, K. 2000, *A&A*, submitted
- Fuhrmann, K., Pfeiffer, M., Frank, C., Reetz, J., & Gehren, T. 1997, *A&A*, 323, 909
- Garnett, D. R., Shields, G. A., Peimber, M., et al. 1999, *ApJ*, 513, 168
- Gehren, T., Butler, K., Mashonkina, L., Reetz, J., & Shi, J. R. 2001, *A&A*, 366, 981
- Gilmore, G. 1995, in *IAU Symp. 164, Stellar Populations*, ed. P. C. van der Kruit, & G. Gilmore (Kluwer, Dordrecht), 99
- Gray, D. F. 1984, *ApJ*, 281, 719
- Gustafsson, B., Karlsson, T., Olsson, E., Edvardsson, B., & Ryde, N. 1999, *A&A*, 342, 426
- Gustafsson, B., & Ryde, N. 2000, in *IAU Symp. 177, The Carbon Star Phenomenon*, ed. R. F. Wing (Kluwer, Dordrecht), 481
- Henry, R. B. C., Edmunds, M. G., & Köppen, J. 2000, *ApJ*, 541, 660
- Hibbert, A., Biémont, E., Godefroid, M., & Vaeck, N. 1991, *A&AS*, 88, 505
- Hibbert, A., Biémont, E., Godefroid, M., & Vaeck, N. 1993, *A&AS*, 99, 179
- Hou, J. L., Prantzos, N., & Boissier, S. 2000, *A&A*, 362, 921
- Karlsson, T., Edvardsson, B., Gustafsson, B., Olsson, E., & Ryde, N. 1999, *APS&S*, 265, 261
- Kobulnicky, H. A., & Skillman, E. D. 1998, *ApJ*, 497, 601
- Kurucz, R. L., Furenlid, I., Brault, J., & Tetzerman, L. 1984, *Solar Flux Atlas from 296 to 1300nm*, Nat. Solar Obs., Sunspot, New Mexico
- Laird, J. B. 1985, *ApJ*, 289, 556
- Leininger, T., Gadéa, F. X., & Dickinson, A. S. 2000, *J. Phys. B, At. Mol. Opt. Phys.*, 32, 283
- Liang, Y. C., Zhao, G., & Shi, J. R. 2001, *A&A*, 374, 936
- Maeder, A. 1992, *A&A*, 264, 105
- Maeder, A., & Meynet, G. 1993, *A&A*, 278, 406
- Maeder, A., & Meynet, G. 2000, *ARA&A*, 38, 143
- Marigo, P. 2001, *A&A*, 370, 194
- Marigo, P., Bressan, A., & Chiosi, C. 1996, *A&A*, 313, 545
- Marigo, P., Bressan, A., & Chiosi, C. 1998, *A&A*, 331, 564
- McWilliam, A. 1997, *ARA&A*, 35, 503
- Oberhummer, H., Csótó, A., & Schlattl, H. 2000, *Science*, 289, 88
- Portinari, L., Chiosi, C., & Bressan, A. 1998, *A&A*, 334, 505
- Prantzos, N., Vangioni-Flam, E., & Chauveaux, S. 1994, *A&A*, 285, 132
- Rentzsch-Holm, I. 1996, *A&A*, 305, 275
- Renzini, A., & Voli, M. 1981, *A&A*, 94, 175
- Ryan, S. G. 1998, *A&A*, 331, 1051
- Stürenburg, S., & Holweger, H. 1990, *A&A*, 237, 125
- Takeda, Y. 1994, *PASJ*, 46, 53
- Timmes, F. X., Woosley, S. E., & Weaver, T. A. 1995, *ApJS*, 98, 617
- Tomkin, J., & Lambert, D. L. 1984, *ApJ*, 279, 220
- Tomkin, J., Lemke, M., Lambert, D. L., & Sneden, C. 1992, *AJ*, 104, 1568
- Tomkin, J., Woolf, V. M., & Lambert, D. L. 1995, *AJ*, 109, 2204
- Twarog, B. A. 1980, *ApJ*, 242, 242
- van den Hoek, L. B., & Groenewegen, M. A. T. 1997, *A&AS*, 123, 305
- Vila-Costas, M. B., & Edmunds, M. G. 1993, *MNRAS*, 265, 199
- Wheeler, J., Sneden, C., & Truran, J. W. 1989, *ARA&A*, 27, 279
- Wielen, R., Fuchs, B., & Dettbarn, C. 1996, *A&A*, 314, 438
- Woosley, S. E., & Weaver, T. A. 1995, *ApJS*, 101, 181